Journal of Power Sources 244 (2013) 336–343

Contents lists available at SciVerse ScienceDirect

Journal of Power Sources

journal homepage: www.elsevier.com/locate/jpowsour

Characteristics of Li_2TiO_3–$LiCrO_2$ composite cathode powders prepared by ultrasonic spray pyrolysis

You Na Ko [a,b], Seung Ho Choi [a], Yun Chan Kang [a,*], Seung Bin Park [b]

[a] Department of Chemical Engineering, Konkuk University, 1 Hwayang-dong, Gwangjin-gu, Seoul 143-701, Republic of Korea
[b] Department of Chemical and Biomolecular Engineering, Korea Advanced Institute of Science and Technology, 291 Daehak-ro, Yuseong-gu, Daejeon 305-701, Republic of Korea

HIGHLIGHTS

- Spherical-shaped Li_2TiO_3–$LiCrO_2$ composite powders are prepared using spray pyrolysis.
- The composite powders have a high initial discharge capacity of 203 mAh g^{-1}.
- The composite powders have good cycle properties due to the stabilizing effect of inactive Li_2TiO_3.

GRAPHICAL ABSTRACT

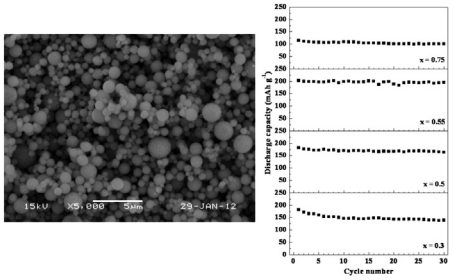

ARTICLE INFO

Article history:
Received 15 October 2012
Received in revised form
15 December 2012
Accepted 3 January 2013
Available online 16 January 2013

Keywords:
Composite cathode
Spray pyrolysis
Lithium battery
Lithium-rich compounds

ABSTRACT

Li_2TiO_3–$LiCrO_2$ cathode powders of various compositions are prepared by spray pyrolysis. Pure Li_2TiO_3 powder and Li_2TiO_3–$LiCrO_2$ composite cathode powder have a spherical shape, nonaggregated structure, and fine sizes even after post-treatment at 700 °C under nitrogen atmosphere. The optimum post-treatment temperature to obtain composite powders with high initial discharge capacity, high coulombic efficiency, and good cycle properties is 700 °C. The initial charge capacities increase when the $LiCrO_2$ content of the composite increase. However, the $0.55Li_2TiO_3$–$0.45LiCrO_2$ composite cathode powders have the highest initial discharge capacity of 203 mAh g^{-1}, in which the capacity retention after 30 cycles is 96%. The dQ/dV curve of the first charge curve has a distinct oxidation peak at approximately 3.9 V, which corresponds to Cr oxidation. The oxidation peak shifts to a lower voltage range at approximately 3.6 V after the first cycling because an irreversible reaction takes place in the initial charge process. The composite cathode powders with low $LiCrO_2$ content have low initial charge/discharge capacities and good cycle properties because of the stabilizing effect of high amounts of an inactive Li_2TiO_3 component.

1. Introduction

The composite Li_2MnO_3–$LiCrO_2$ draws wide attention because of its high capacity and good cyclability, which are attributed to the three-electron redox couple of Cr^{3+}/Cr^{6+} rather than to Mn [1–5]. In the Li_2MnO_3–$LiCrO_2$ composite, Mn ions exist in a 4^+ oxidation state, an electrochemically inactive state, which serves to stabilize the layered composite materials. In addition to Li_2MnO_3, Li_2TiO_3 is applied to stabilize the $LiCrO_2$ component [6,7]. Li_2TiO_3, which is isostructural to Li_2MnO_3 and has a strong Ti–O bond relative to Mn–O, can remarkably stabilize the layered $LiCrO_2$ cathode components [8–11].

The dispersion of layered Li_2MnO_3 phase in layered $LiMO_2$ (M = Ni, Co, and Mn) matrix needs to be uniform and fine in order to improve the electrochemical properties of the composite

* Corresponding author. Tel.: +82 2 2049 6010; fax: +82 2 458 3504.
E-mail address: yckang@konkuk.ac.kr (Y.C. Kang).

0378-7753/$ – see front matter © 2013 Elsevier B.V. All rights reserved.
http://dx.doi.org/10.1016/j.jpowsour.2013.01.027

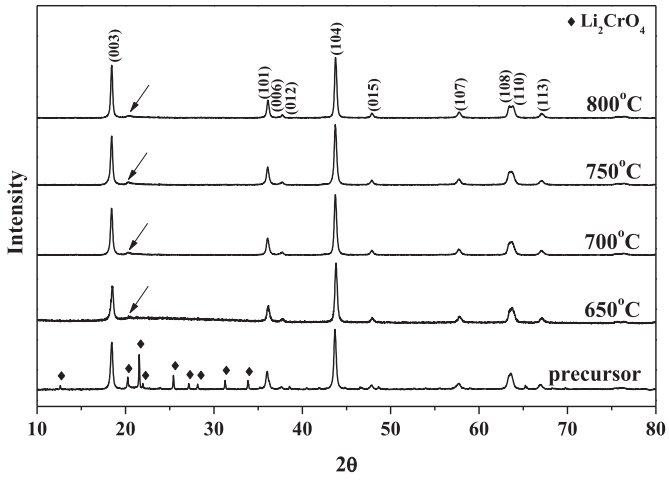

Fig. 1. XRD patterns of the precursor and post-treated Li_2TiO_3–$LiCrO_2$ powders.

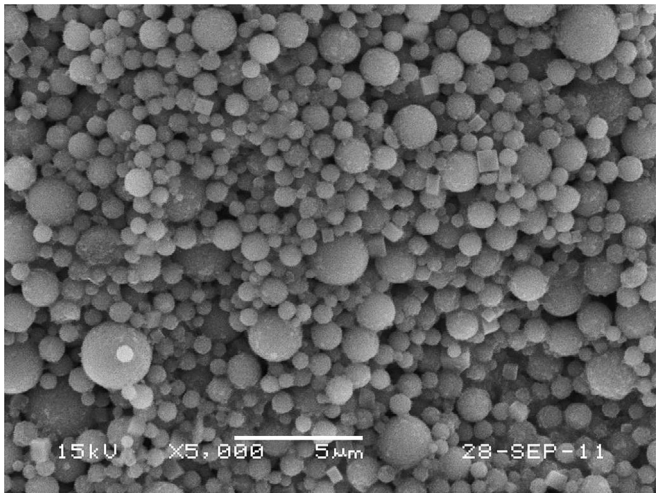

Fig. 2. SEM image of the precursor powders prepared by spray pyrolysis.

cathode materials [12,13]. Therefore, the capacities and cycle properties of the composite cathode materials are strongly affected by the methods used to prepare the composite cathode powders [12–18]. However, the characteristics of the Li_2TiO_3–$LiCrO_2$ composite powders have been scarcely studied using well-established methods such as solid-state reaction and sol–gel processes [11,19,20].

It is well known that spherical cathode materials are advantageous to obtaining a high tap density and excellent electrochemical

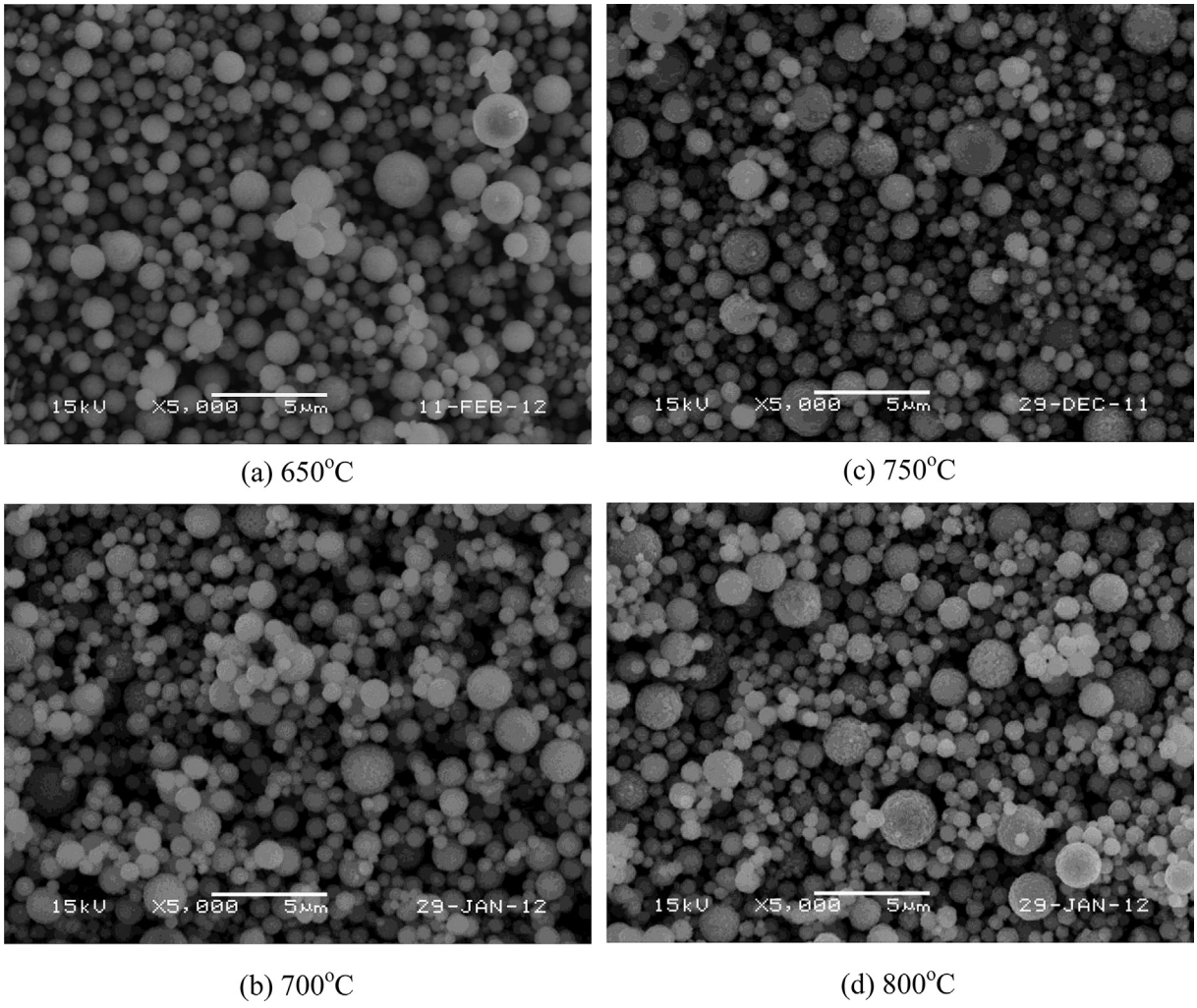

Fig. 3. SEM images of the $0.55Li_2TiO_3$–$0.45LiCrO_2$ composite powders post-treated at various temperatures.

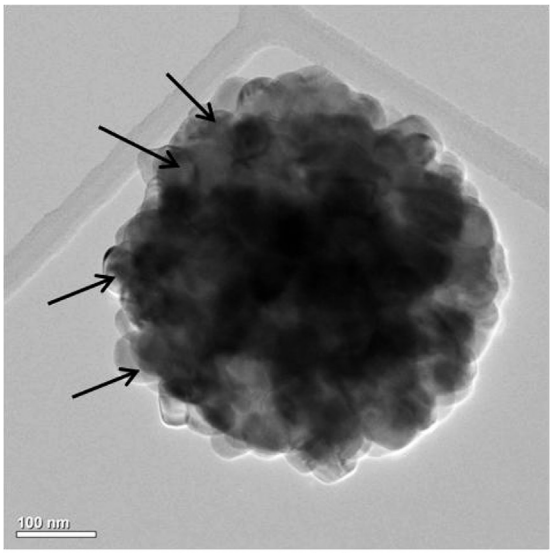

(a) low resolution

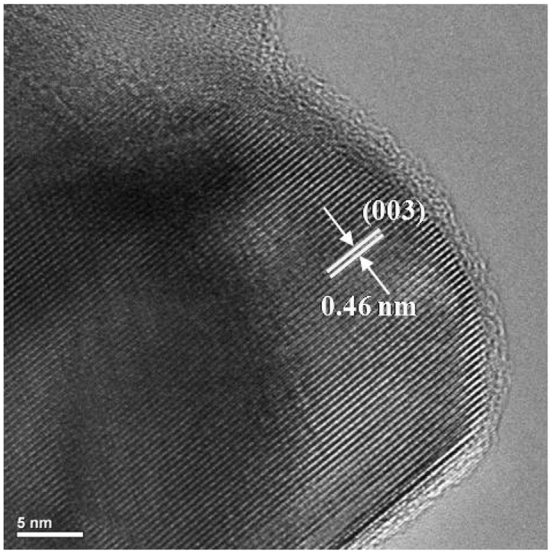

(b) high resolution

Fig. 4. TEM images of the $0.55Li_2TiO_3$–$0.45LiCrO_2$ composite powders post-treated at 700 °C.

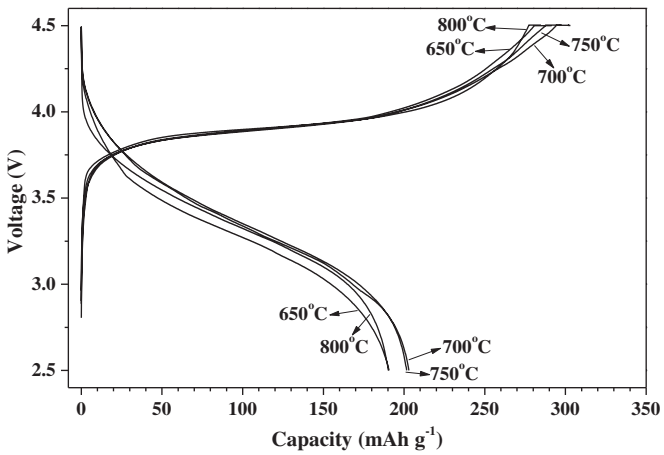

Fig. 5. Initial charge/discharge curves of the $0.55Li_2TiO_3$–$0.45LiCrO_2$ composite powders post-treated at various temperatures.

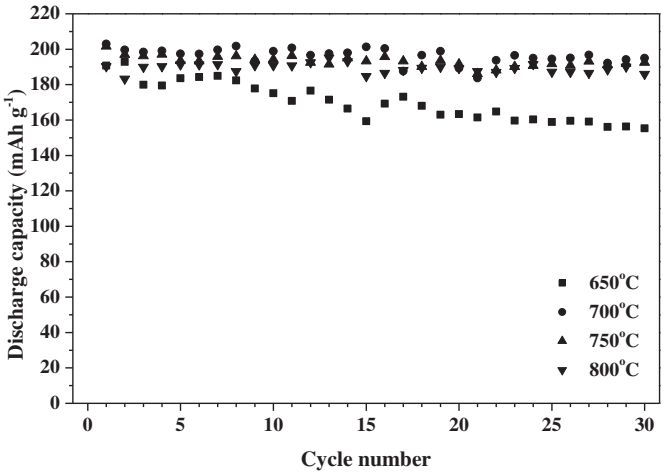

Fig. 6. Cycle properties of the $0.55Li_2TiO_3$–$0.45LiCrO_2$ composite powders post-treated at various temperatures.

properties [21–24]. However, the characteristics of spherical Li_2MO_3–$LiCrO_2$ composite powders have not been studied. Morphological control is obscured by the formation of a Li_2CrO_4 impurity phase during the preparation of Li_2MO_3–$LiCrO_2$ composite powders [5,25]. Spray pyrolysis, which is one of the gas-phase reaction methods, is a good alternative method for the preparation of powders with uniform compositions and a spherical shape [26–28]. Spray pyrolysis applying an ultrasonic nebulizer is already commercialized in large-scale production of various types of ceramic and metal powders. Ko et al. prepared nano-sized $LiCrO_2$–Li_2MnO_3 composite powders by a new modified spray pyrolysis process. The powders have a pure layered structure similar to that of the $LiCrO_2$–Li_2MnO_3 composite after Li_2CrO_4 is removed by washing with distilled water [29].

In this study, spherical $xLi_2TiO_3 - (1 - x)LiCrO_2$ ($x = 0$, 0.3, 0.5, 0.55, 0.75, and 1) composite powders are prepared by spray pyrolysis. The effects of the ratios of the Li_2TiO_3 and $LiCrO_2$ phases on the physical and electrochemical properties of the composite powders are investigated.

2. Experimental

The $xLi_2TiO_3 - (1 - x)LiCrO_2$ composite cathode materials were prepared by spray pyrolysis. The equipment used consisted of

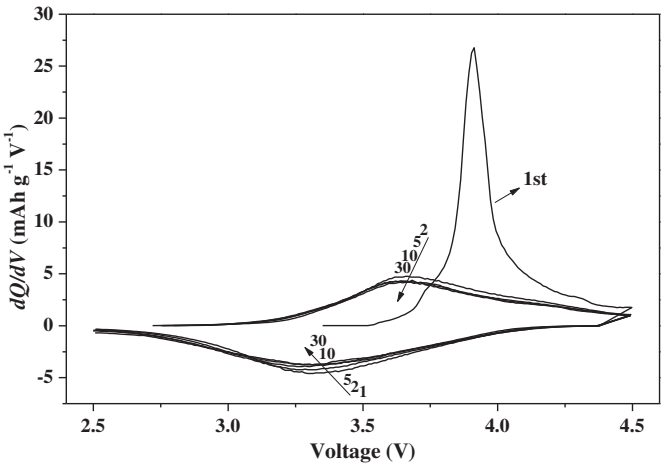

Fig. 7. Differential capacity vs. voltage (dQ/dV) curves of the $0.55Li_2TiO_3$–$0.45LiCrO_2$ composite powders post-treated at 700 °C.

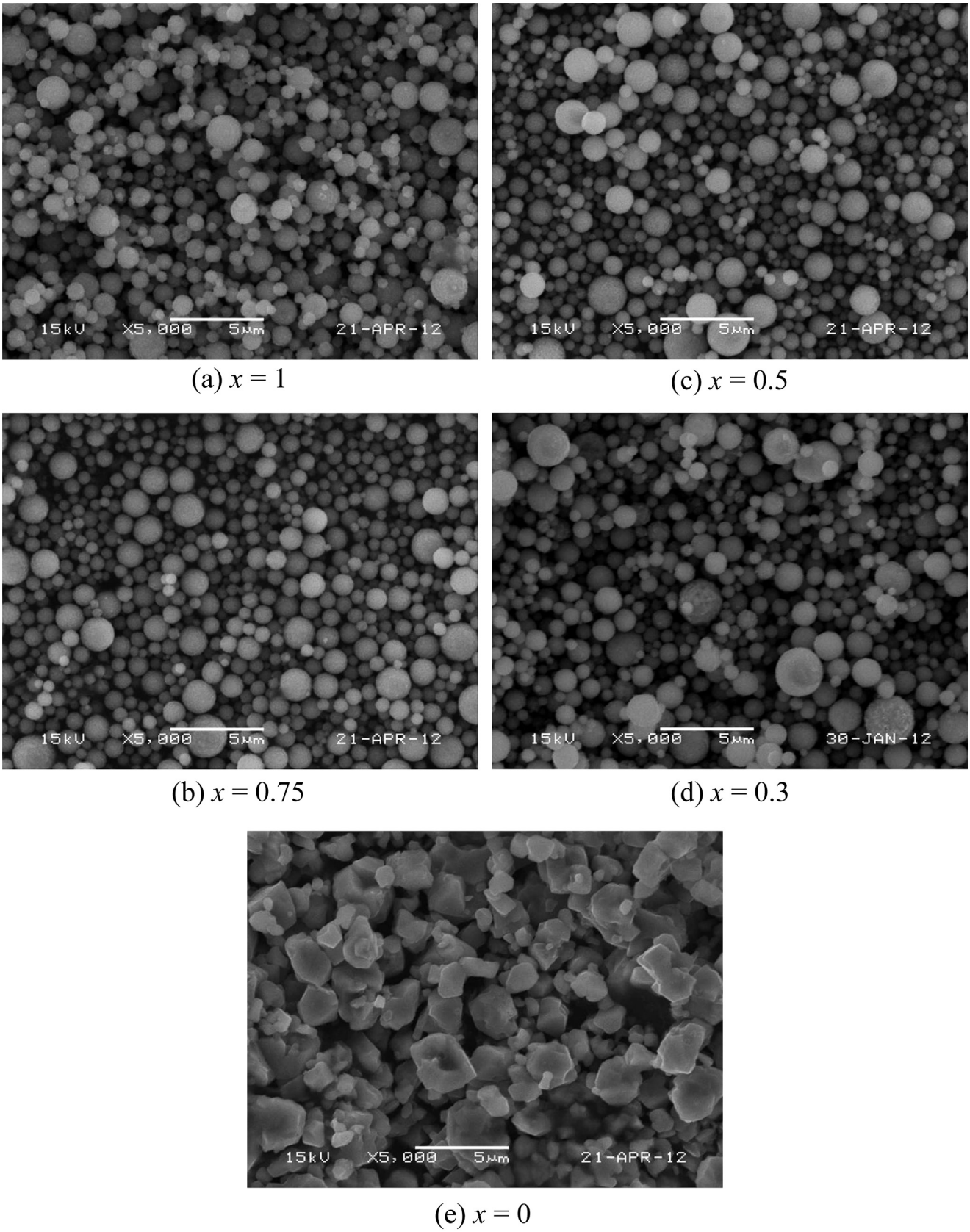

Fig. 8. SEM images of the xLi_2TiO_3–$(1 - x)LiCrO_2$ powders with varying values of x post-treated at 700 °C.

a quartz reactor, a bag filter, and six ultrasonic spray generators operating at 1.7 MHz. The length and diameter of the quartz reactor were 1000 and 50 mm, respectively. The preparation temperature and the flow rate of air used as the carrier gas were fixed at 1000 °C and 10 L min^{-1}. The starting materials were lithium nitrate, chromium nitrate nonahydrate, and titanium tetraisopropoxide (TTIP). A small amount of nitric acid was used to peptize the hydrolyzed TTIP and form a clear solution. The concentration of metal components in the spray solution was fixed at 0.5 M, and a lithium component in excess of 5 wt% of the stoichiometric amount was added. The value of x in $xLi_2TiO_3 - (1 - x)LiCrO_2$ was varied from 0 to 1. The precursor powders obtained by spray pyrolysis were post-treated at various temperatures from 650 to 800 °C for 12 h in nitrogen atmosphere.

The morphologies of the precursor and post-treated cathode powders were investigated by scanning electron microscopy (SEM, JEOL JSM-6060) and transmission electron microscopy (TEM, JEOL JEM-2010). The crystal structures of the powders were investigated by X-ray diffractometry (XRD, X'Pert PRO MPD) using Cu Kα radiation ($\lambda = 1.5418$ Å) at the Korea Basic Science Institute (Daegu). The electrochemical properties of the prepared Li_2TiO_3–$LiCrO_2$ composite powders were tested in a 2032-type coin cell. The cathode powder was prepared from a mixture of 20 mg composite powders and 12 mg TAB (TAB is a mixture of 9.6 mg teflonized acetylene black and 2.4 mg binder). Lithium metal and a microporous polypropylene film were used as the anode and separator, respectively. The electrolyte was 1 M $LiPF_6$ in a 1:1 mixture by volume of ethylene carbonate/dimethyl carbonate (EC/DMC). The cells were tested in the 2.5–4.5 V potential range at a constant current density of 15 mA g^{-1}.

3. Results and discussion

The crystal structures of the precursors and post-treated $0.55Li_2TiO_3$–$0.45LiCrO_2$ composite powders are shown in Fig. 1. The precursor powders obtained directly by spray pyrolysis under an air atmosphere were post-treated at various temperatures under nitrogen atmosphere. The precursor powders had mixed crystal structures of layered α-$NaFeO_2$ structure and an impurity phase of Li_2CrO_4, which impurity was formed by reaction of lithium and chromium components in air atmosphere. Therefore, the precursor powders were post-treated under nitrogen atmosphere to form the Li_2TiO_3–$LiCrO_2$ composite structure without impurities. After post-treatment, the powders had a mixed-layer crystal structure consisting of Li_2TiO_3 and $LiCrO_2$ phases, irrespective of the post-treatment temperatures. The XRD patterns of the post-treated powders showed a superlattice peak near 21°, as indicated by the arrows in Fig. 1, which correspond to the short-range ordering of Li, Cr, and Ti atoms in the transition metal layers [10,30]. The splitting peaks of (108) and (110) indicate that the samples have a layered structure.

The morphology of the precursor powders for the $0.55Li_2TiO_3$–$0.45LiCrO_2$ composite obtained by spray pyrolysis is shown in Fig. 2. The precursor powders had a spherical shape and a size on the order of microns because they were formed from one droplet by drying, decomposition, and crystallization processes inside the hot wall reactor. Slight aggregation between the precursor powders with a spherical shape occurred because Li_2CrO_4 has a high solubility in water. The melting of Li_2CrO_4 by adsorption of water molecules resulted in aggregated precursor powders. Fig. 3 shows the $0.55Li_2TiO_3$–$0.45LiCrO_2$ composite powders post-treated at temperatures between 650 and 800 °C. The composite powders had a spherical shape and nonaggregated characteristics, irrespective of the post-treatment temperatures. The conversion of the water-soluble Li_2CrO_4 phase to a stable $LiCrO_2$ phase changed the morphology of the post-treated composite powders. The composite powders post-treated at a low temperature of 650 °C had a smooth surface. However, the roughness of the surface of the composite powders increased with increasing post-treatment temperature because of crystal growth. The mean sizes of the composite powders post-treated at 700 °C measured, as from the SEM images, were 0.92 μm. Fig. 4 shows the TEM images of the composite powders post-treated at 700 °C. The micron-sized Li_2TiO_3–$LiCrO_2$ powders were composed of nanosized crystals, as shown by the arrows in the low resolution TEM image in Fig. 4(a). The high-resolution TEM image exhibits clear lattice fringes with a separation of 0.46 nm. This value corresponds to the (003) plane of $LiCrO_2$ having an α-$NaFeO_2$-layered structure [31,32].

The electrochemical properties of the $0.55Li_2TiO_3$–$0.45LiCrO_2$ composite cathode powders post-treated at various temperatures were investigated in the voltage range 2.5–4.5 V at a constant current density of 15 mA g^{-1} Figs. 5 and 6 show the initial charge/discharge curves and the cycle properties of the composite cathode powders post-treated at various temperatures. The composite powders had similar charge/discharge curves, irrespective of the post-treatment temperature. The initial discharge capacities of the cathode powders were 191, 203, 202, and 190 mAh g^{-1} when the post-treatment temperatures were 650, 700, 750, and 800 °C, respectively. The Coulombic efficiencies of the first cycles of the composite cathode powders were about 67%, irrespective of the post-treatment temperature. However, the cycle properties of the composite cathode powders were affected by the post-treatment temperature, as shown in Fig. 6. The discharge capacities of the composite powders post-treated at 650, 700, 750, and 800 °C decreased from 191, 203, 202, and 190 mAh g^{-1} to 155, 195, 193, and 186 mAh g^{-1}, respectively, after the 30th cycle. The capacity retentions of the composite powders post-treated at 650, 700, 750, and 800 °C were 81, 96, 96, and 98%, respectively. The cyclabilities

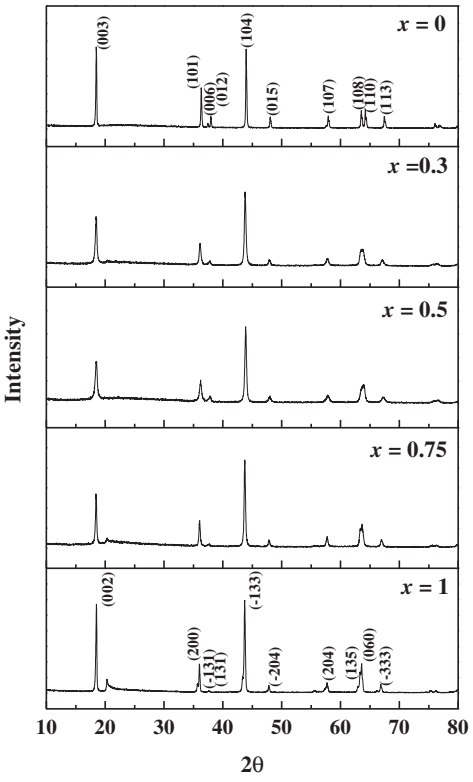

Fig. 9. XRD patterns of the xLi_2TiO_3–$(1 - x)LiCrO_2$ powders with varying values of x post-treated at 700 °C.

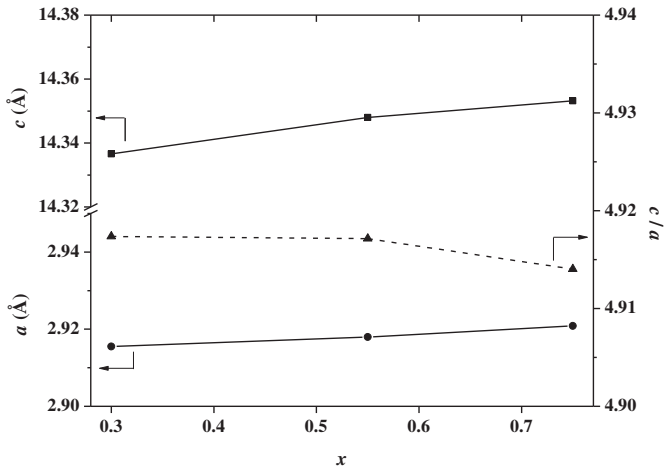

Fig. 10. Lattice parameters and axis ratio values of the xLi$_2$TiO$_3$–(1 – x)LiCrO$_2$ composite powders with varying values of x.

of the composite powders improved with increasing post-treatment temperature. The 0.55Li$_2$TiO$_3$–0.45LiCrO$_2$ composite powders post-treated at 700 °C had the highest initial charge and discharge capacities and good cycle properties.

Fig. 7 shows the differential capacity versus voltage curves (dQ/dV) of the 0.55Li$_2$TiO$_3$–0.45LiCrO$_2$ composite powders post-treated at 700 °C. The first charge curve had a distinct oxidation peak around 3.9 V. This peak indicates that the presence of a plateau in the initial charge curve in the voltage range near 3.9 V, as shown in Fig. 5, is related to the Cr oxidation [33]. The oxidation peak observed in the first charge curve shifted to a low-voltage range around 3.6 V after the first cycle because an irreversible reaction takes place in the initial charge process. During the first cycle, some Cr^{3+} ions irreversibly move to the octahedral sites in the lithium layer, and this process causes the high irreversible capacity loss, shown in Fig. 5 [6,20]. The oxidation/reduction peaks around 3.6/3.2 V are associated with the Cr^{3+}/Cr^{6+} redox couple. The shape of the dQ/dV curves was almost stable after the second cycle. Therefore, the 0.55Li$_2$TiO$_3$–0.45LiCrO$_2$ composite cathode powders post-treated at 700 °C had good cycle properties, as shown in Fig. 6.

The physical and electrochemical properties of pure Li$_2$TiO$_3$ and LiCrO$_2$ powders and the Li$_2$TiO$_3$–LiCrO$_2$ composite cathode powder were investigated. The precursor powders prepared directly by spray pyrolysis were post-treated at 700 °C for 12 h under nitrogen

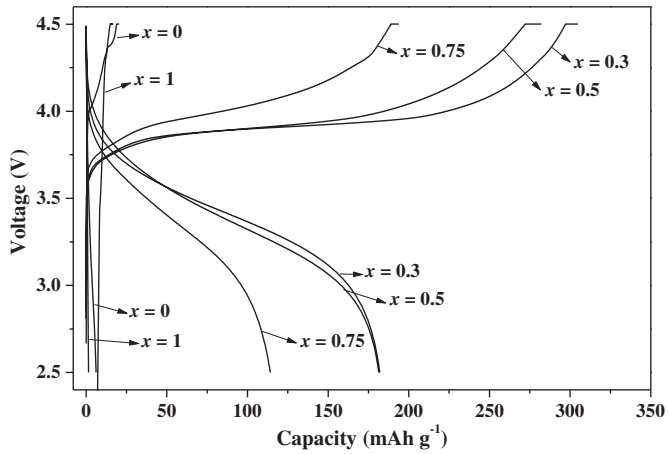

Fig. 11. Initial charge/discharge curves of the xLi$_2$TiO$_3$–(1 – x)LiCrO$_2$ composite powders with varying values of x.

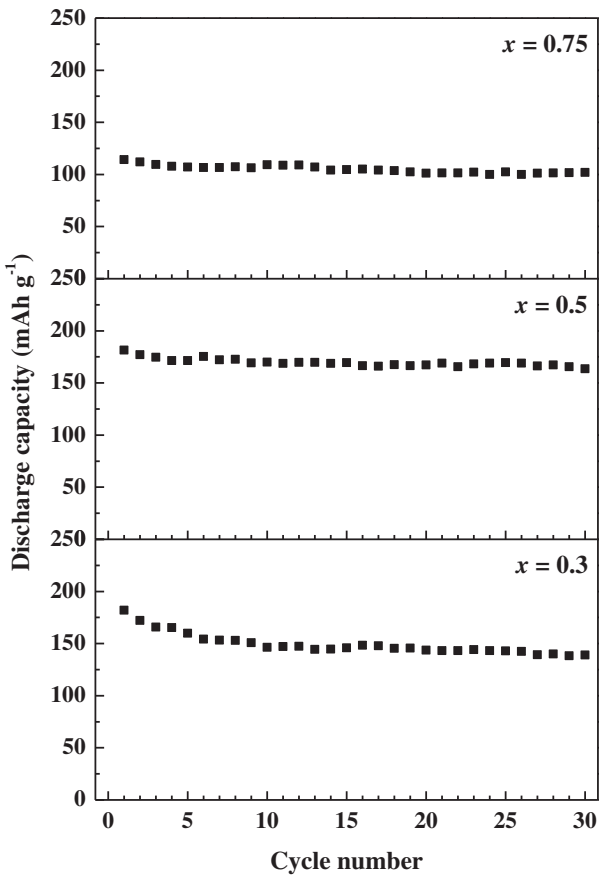

Fig. 12. Cycle properties of the xLi$_2$TiO$_3$–(1 – x)LiCrO$_2$ composite powders with varying values of x.

atmosphere. Fig. 8 shows the morphologies of the post-treated pure and composite cathode powders. The precursor powders had a spherical shape and sizes on the order of microns, irrespective of the composition of the cathode powders. After post-treatment at 700 °C, the pure Li$_2$TiO$_3$ powder and the Li$_2$TiO$_3$–LiCrO$_2$ composite cathode powder retained their spherical shapes, nonaggregated structures, and fine sizes, while the pure LiCrO$_2$ powder transformed to nonspherical shapes with large sizes. The

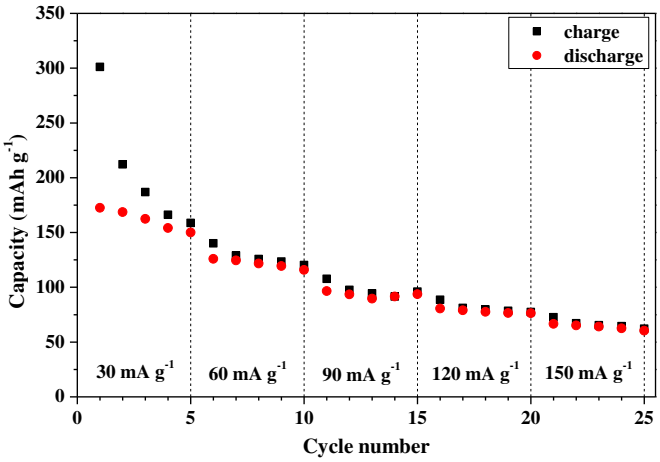

Fig. 13. Rate performances of the 0.55Li$_2$TiO$_3$–0.45LiCrO$_2$ composite powders post-treated at 700 °C.

Table 1
Electrochemical properties of Li_2TiO_3–$LiCrO_2$ prepared by various methods.

Synthesis method	Composition	Voltage range (V)	Current density (mA g^{-1})	Discharge capacity (mAh g^{-1})	Ref
Solid–state reaction	$LiCrO_2$–Li_2TiO_3 (Ti/(Ti + Cr) = 0.5)	2.0–4.8	8	173	[11]
			160	101	
Solid–state reaction	Li–Cr–Ti–O (Li/(Cr + Ti) = 1.5)	2.0–4.8	32	152	[19]
Sol–gel method	$Li[Cr_xLi_{(1/3-x/3)}Ti_{(2/3-2x/3)}]O_2$/C ($x$ = 0.35)	2.5–4.4	30	150	[20]
			150	75	
Present work	$0.55Li_2TiO_3$–$0.45LiCrO_2$	2.5–4.5	15	203	–

composite powders had similar mean sizes because one particle was formed from one droplet, irrespective of the composition of the powders.

Fig. 9 shows the XRD patterns of the pure Li_2TiO_3 and $LiCrO_2$ powders and the Li_2TiO_3–$LiCrO_2$ composite cathode powders post-treated at 700 °C. The Li_2TiO_3 and $LiCrO_2$ powders had single phases without any impurity peaks. As the $LiCrO_2$ content increased, the superlattice peak near 21° became weaker because Li, which is located in the transition-metal layer, was reduced [11,20]. The variations in the lattice parameters a and c and the c/a ratio with respect to the compositions of the composite powders are shown in Fig. 10. As the $LiCrO_2$ content increased, the lattice parameters a and c of the composite powders decreased. The c/a ratios of the composite powders are higher than 4.9. This result shows that the composite powders prepared by spray pyrolysis have the structural properties of layered materials [13,34,35].

The initial charge/discharge curves and cycle properties of the pure Li_2TiO_3 and $LiCrO_2$ powders and the Li_2TiO_3–$LiCrO_2$ composite cathode powders were determined in the voltage range 2.5–4.5 V at a constant current density of 15 mA g^{-1}, and the results are shown in Figs. 11 and 12. The pure Li_2TiO_3 and $LiCrO_2$ cathode powders had low initial charge and discharge capacities. The initial charge/discharge curves of the Li_2TiO_3–$LiCrO_2$ composite cathode powders are quite similar in shape, irrespective of the compositions. Large, irreversible capacity losses in the initial cycles, which are typical of a "layered–layered" composite electrode, are observed in all composite cathode powders. The initial irreversible capacity losses increased with increasing $LiCrO_2$ content of the composite powders. The irreversible capacity losses of the $0.75Li_2TiO_3$–$0.25LiCrO_2$ and $0.3Li_2TiO_3$–$0.7LiCrO_2$ composite cathode powders are 80 and 123 mAh g^{-1}, respectively. The initial charge capacities increased with increasing $LiCrO_2$ content of the composite powders because only chromium acts as a redox couple upon cycling in the composite powders. However, the $0.55Li_2TiO_3$–$0.45LiCrO_2$ composite cathode powders had the highest initial discharge capacity of 203 mAh g^{-1}. The composite cathode powders with low $LiCrO_2$ content had low initial charge/discharge capacities and good cycle properties because of the stabilizing effect of high amounts of an inactive Li_2TiO_3 component [20].

The rate performances of the $0.55Li_2TiO_3$–$0.45LiCrO_2$ composite powders post-treated at 700 °C were measured between 2.5 and 4.5 V when the charge/discharge rate increased from 30 to 150 mA g^{-1} in a step-by-step manner (see Fig. 13). The first discharge capacity of the composite powders was 173 mAh g^{-1} at constant charge and discharge rate of 30 mA g^{-1}. The discharge capacity gradually decreased with increasing charge and discharge rate. The electrochemical properties of the prepared Li_2TiO_3–$LiCrO_2$ composite powders were compared to those of powders with similar compositions previously reported in the literature. The results of the previous reports are summarized in Table 1. The composite powders prepared by spray pyrolysis had higher capacities than those prepared by solid-state reaction and sol–gel methods because of their fine size and phase homogeneity. However, the Li_2TiO_3–$LiCrO_2$–C composite powders prepared by the sol–gel method had better cycle retention at high charge and discharge rates than do the Li_2TiO_3–$LiCrO_2$ composite powders prepared by spray pyrolysis. The composition should thus be optimized to improve the rate performances of the Li_2TiO_3–$LiCrO_2$ composite powders prepared using spray pyrolysis.

4. Conclusions

Spherical $xLi_2TiO_3 - (1 - x)LiCrO_2$ composite cathode powders were prepared by spray pyrolysis. The spherical shape and fine size of the precursor powders obtained by spray pyrolysis were maintained even after post-treatment at temperatures between 650 and 800 °C under nitrogen atmosphere. The precursor powders had mixed crystal structures of layered α-$NaFeO_2$ phase and an impurity Li_2CrO_4 phase. The post-treated powders had a mixed-layered crystal structure consisting of Li_2TiO_3 and $LiCrO_2$ phases, irrespective of the post-treatment temperature. The initial charge/discharge curves of the Li_2TiO_3–$LiCrO_2$ composite cathode powders are quite similar in shape, irrespective of the compositions. The initial charge capacities and initial irreversible capacity losses increased with increasing $LiCrO_2$ content of the composite powders because only chromium acts as a redox couple on cycling in the composite powders. However, the $0.55Li_2TiO_3$–$0.45LiCrO_2$ composite cathode powders had the highest initial discharge capacity of 203 mAh g^{-1} and good cycle properties because of the stabilizing effect of the inactive Li_2TiO_3 component.

Acknowledgment

This work was supported by the National Research Foundation of Korea (NRF) grant funded by the Korea government (MEST) (No. 2012R1A2A2A02046367). This work was supported by Seoul R&BD Program (WR090671).

References

[1] C.W. Park, S.H. Kim, K.S. Nahm, H.T. Chung, Y.S. Lee, J.H. Lee, S. Boo, J. Kim, J. Alloys Compd 449 (2008) 343.
[2] Z. Lu, J.R. Dahn, J. Electrochem. Soc. 149 (2002) A1454.
[3] X. Wu, S.H. Chang, Y.J. Park, K.S. Ryu, J. Power Sources 137 (2004) 105.
[4] B. Ammundsen, J. Paulsen, I. Davidson, R.S. Liu, C.H. Shen, J.M. Chen, L.Y. Jang, J.F. Lee, J. Electrochem. Soc. 149 (2002) A431.
[5] C.W. Park, S.H. Kim, I.R. Mangani, J.H. Lee, S. Boo, J. Kim, Mater. Res. Bull. 42 (2007) 1374.
[6] M. Balasubramanian, J. McBreen, I.J. Davidson, P.S. Whitfield, I. Kargina, J. Electrochem. Soc. 149 (2002) A176.
[7] Z. Lu, Z. Chen, J.R. Dahn, Chem. Mater. 15 (2003) 3214.
[8] J.S. Kim, C.S. Johnson, M.M. Thackeray, Electrochem. Commun. 4 (2002) 205.
[9] C.S. Johnson, J.S. Kim, A.J. Kropf, A.J. Kahaian, J.T. Vaughey, M.M. Thackeray, J. Power Sources 119-121 (2003) 139.
[10] J.S. Kim, C.S. Johnson, J.T. Vaughey, M.M. Thackeray, S.A. Hackney, W. Yoon, C.P. Grey, Chem. Mater. 16 (2004) 1996.
[11] L. Zhang, H. Noguchi, J. Electrochem. Soc. 150 (2003) A601.
[12] F. Wu, H. Lu, Y. Su, N. Li, L. Bao, S. Chen, J. Appl. Electrochem 40 (2010) 783.
[13] P.S. Whitfield, S. Niketic, I.J. Davidson, J. Power Sources 146 (2005) 617.
[14] C.S. Johnson, J.S. Kim, C. Lefief, N. Li, J.T. Vaughey, M.M. Thackeray, Electrochem. Commun. 6 (2004) 1085.
[15] B.L. Ellis, K.T. Lee, L.F. Nazar, Chem. Mater. 22 (2010) 691.

[16] J.S. Kim, C.S. Johnson, J.T. Vaughey, M.M. Thackeray, J. Power Sources 153 (2006) 258.
[17] H. Deng, I. Belharouak, R.E. Cook, H. Wu, Y.K. Sun, K. Amine, J. Electrochem. Soc. 157 (2010) A447.
[18] T. Ohzuku, M. Nagayama, K. Tsuji, K. Ariyoshi, J. Mater. Chem. 21 (2011) 10179.
[19] L. Zhang, H. Noguchi, Electrochem. Commun. 4 (2002) 560.
[20] X. Mi, H. Li, X. Huang, J. Power Sources 174 (2007) 867.
[21] S.K. Hu, G.H. Cheng, M.-Y. Cheng, B.J. Hwang, R. Santhanam, J. Power Sources 188 (2009) 564.
[22] P. He, H. Wang, L. Qi, T. Osaka, J. Power Sources 160 (2006) 627.
[23] Z. Wang, S. Su, C. Yu, Y. Chen, D. Xia, J. Power Sources 184 (2008) 633.
[24] S.Y. Yang, X.Y. Wang, Z.L. Liu, Q.Q. Chen, X.K. Yang, Q.L. Wei, Trans. Nonferrous Met. Soc. China 21 (2011) 1995.
[25] Y.-K. Sun, M.G. Kim, S.H. Kang, K. Amine, J. Mater. Chem. 13 (2003) 319.
[26] Y.N. Ko, H.Y. Koo, J.H. Kim, J.H. Yi, Y.C. Kang, J.H. Lee, J. Power Sources 196 (2011) 6682.
[27] I. Taniguchi, D. Song, M. Wakihara, J. Power Sources 109 (2002) 333.
[28] S.H. Park, Y.K. Sun, Electrochim. Acta 50 (2004) 431.
[29] Y.N. Ko, J.H. Kim, J.K. Lee, Y.C. Kang, J.H. Lee, Electrochim. Acta 69 (2012) 345.
[30] C.J. Pan, Y.J. Lee, B. Ammundsen, C.P. Grey, Chem. Mater. 14 (2002) 2289.
[31] H.Z. Zhang, Q.Q. Qiao, G.R. Li, S.H. Ye, X.P. Gao, J. Mater. Chem. 22 (2012) 13104.
[32] H.K. Song, K.T. Lee, M.G. Kim, L.F. Nazar, J. Cho, Adv. Funct. Mater. 20 (2010) 3818.
[33] S.T. Myung, S. Komaba, N. Hirosaki, N. Kumagai, Electrochem. Commun. 4 (2002) 397.
[34] Y. Sun, C. Quyang, Z. Wang, X. Huang, L. Chen, J. Electrochem. Soc. 151 (2004) A504.
[35] L. Zhang, K. Takada, N. Ohta, K. Fukuda, T. Sasaki, J. Power Sources 146 (2005) 598.